

NDACC activities of JPL FTIR Instrument



Geoff Toon, Jean-Francois Blavier, Keeyoon Sung
Jet Propulsion Laboratory, California Institute of Technology



MkIV is primarily a balloon instrument. Between flights, it takes ground-based observations from various sites.

Not a primary NDACC instrument/site, but dataset is still useful.

~1100 days of ground observations, 23 balloon flights, and 30+ aircraft flights.

Ground-based dataset has many interruptions due to balloon/aircraft campaigns.

INFRARED WORKING GROUP SITE LOCATIONS

Physical Map of the World, April 2005



With Kitt Peak now defunct, MkIV is the only NDACC-IRWG FTS in continental USA

https://www2.ucar.edu/irwg/barcroft

Home About Sections Observations Modeling Publications Events Opportunities People For Staff

NDACC Infrared Working Group

IRWG SITES GROUPS MEETINGS CONTACTS LINKS SUPPORT

Google Custom Search Search

Home » Barcroft

BARCROFT

Principal Investigator: **Geoffrey Toon**
Institute: **Jet Propulsion Laboratory / NASA**

No Recent Data
No NDACC Data

< Back to clickable world map.

37°34'59.5"N 118°14'54.6"W
View larger map
Directions Save

White Mountain Peak
Chaffant Valley
Dyer
Piper
Camp
Dart

Despite UCAR website saying “No NDACC Data”, there is in fact a large file on the NDACC archive covering nearly all MkIV ground-based results from 1985 to 2015 (see below).

← → ↺ http://ftp.cpc.ncep.noaa.gov/ndacc/station/barcroft/ames/ftir/

Index of /ndacc/station/barcroft/ames/ftir

Name	Last modified	Size
Parent Directory	-	
mbtc8506.tof	08-Apr-2015 17:36	4.2M

← → ↺ http://ftp.cpc.ncep.noaa.gov/ndacc/station/barcroft/ames/ftir/mbtc8506.tof

```

TOON G. C.      FTIR      MT BARCROFT TOTALCOL      17-JUN-1985 00:00:0026-DEC-2014
              310      1001
Toon, Geoffrey (Geoffrey.C.Toon@jpl.nasa.gov, 818 354 8259)
Jet Propulsion Laboratory
JPL MkIV Interferometer
NDACC-IRWG Ground-based Mid-IR column measurements (1985 - 2014)
1 1
1985 06 17      2014 12 26
0.0
record_#
  
```

MkIV Ground-based Dataset

A single file covering 30 years, 12 measurement locations (78S to 68N) & 26 gases

Barcroft is the site with the most observations (hence station name).

Analysis covers 1985 to 2015 with ~1100 observation days

All data measured with same instrument (BS, detectors, etc) and analyzed with the same GGG/TCCON methodology (I2S, GFIT, ATM15 linelist, etc)

Column retrievals of: H₂O, CO₂, O₃, N₂O, CO, CH₄, NO, NO₂, NH₃, HNO₃, HCl, HF, OCS, H₂CO, ClNO₃, HCN, CCl₂F₂, COF₂, C₂H₆, N₂, CHClF₂, HCOOH, HDO, SF₆, C₃H₈ plus various isotopes

Data file is on NDACC archive:

<http://ftp.cpc.ncep.noaa.gov/ndacc/station/barcroft/ames/ftir/mbtc8506.tof>

Also available from:

<http://mark4sun.jpl.nasa.gov/ground.html>

All results shown here are from this file.

MkIV Observation Site Locations

Location	Key	Nobs	Latitude (deg.)	Longitude (deg.)	Altitude (km)
Esrang, Sweden	ESN	160	+67.889	+21.085	0.271
Ft Wainwright, Fairbanks, Alaska	FAI	124	+64.830	-147.614	0.182
Lynn Lake, Manitoba, Canada	LYL	20	+56.858	-101.066	0.354
Mt. Barcroft, California	MTB	1369	+37.584	-118.235	3.801
ARC, Mountain View, California	ARC	7	+37.430	-122.080	0.010
Daggett, California	DAG	33	+34.856	-116.790	0.626
Ft Sumner, New Mexico	FTS	172	+34.480	-104.220	1.260
TMF, Wrightwood, California	TMF	475	+34.382	-117.678	2.257
JPL B183, Pasadena, California	JPL	758	+34.199	-118.174	0.345
JPL Mesa, Pasadena, California	JPL	20	+34.205	-118.171	0.460
NSBF, Palestine, Texas	PAL	4	+31.780	-95.700	0.100
McMurdo, Antarctica	MCM	37	-77.847	+166.728	0.100

Nobs = Number of Observations; +ve Latitude = N; +ve Longitude = E

MkIV dataset is unique in the sense that the same instrument and analysis method has been applied to 12 different locations, minimizing site-to-site biases.

MkIV activities pertaining to NDACC

Continue monitoring atmospheric trace gases

- multiple sites hamper trend evaluation
- Latitude/altitude changes must somehow be accounted for

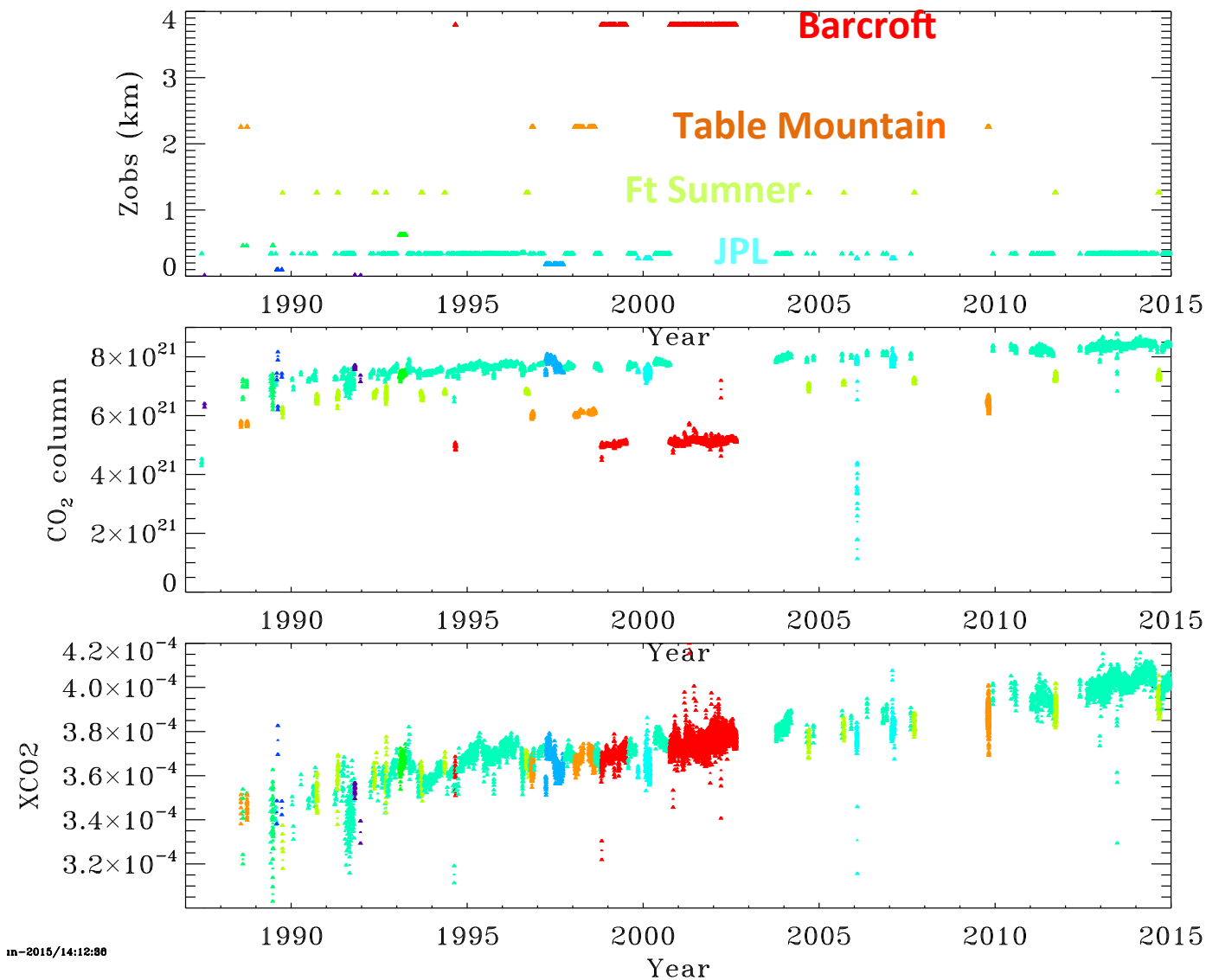
Participate in inter-comparison activities (e.g. MOHAVE)

Investigate feasibility of retrieving new gases (e.g. C_3H_8)

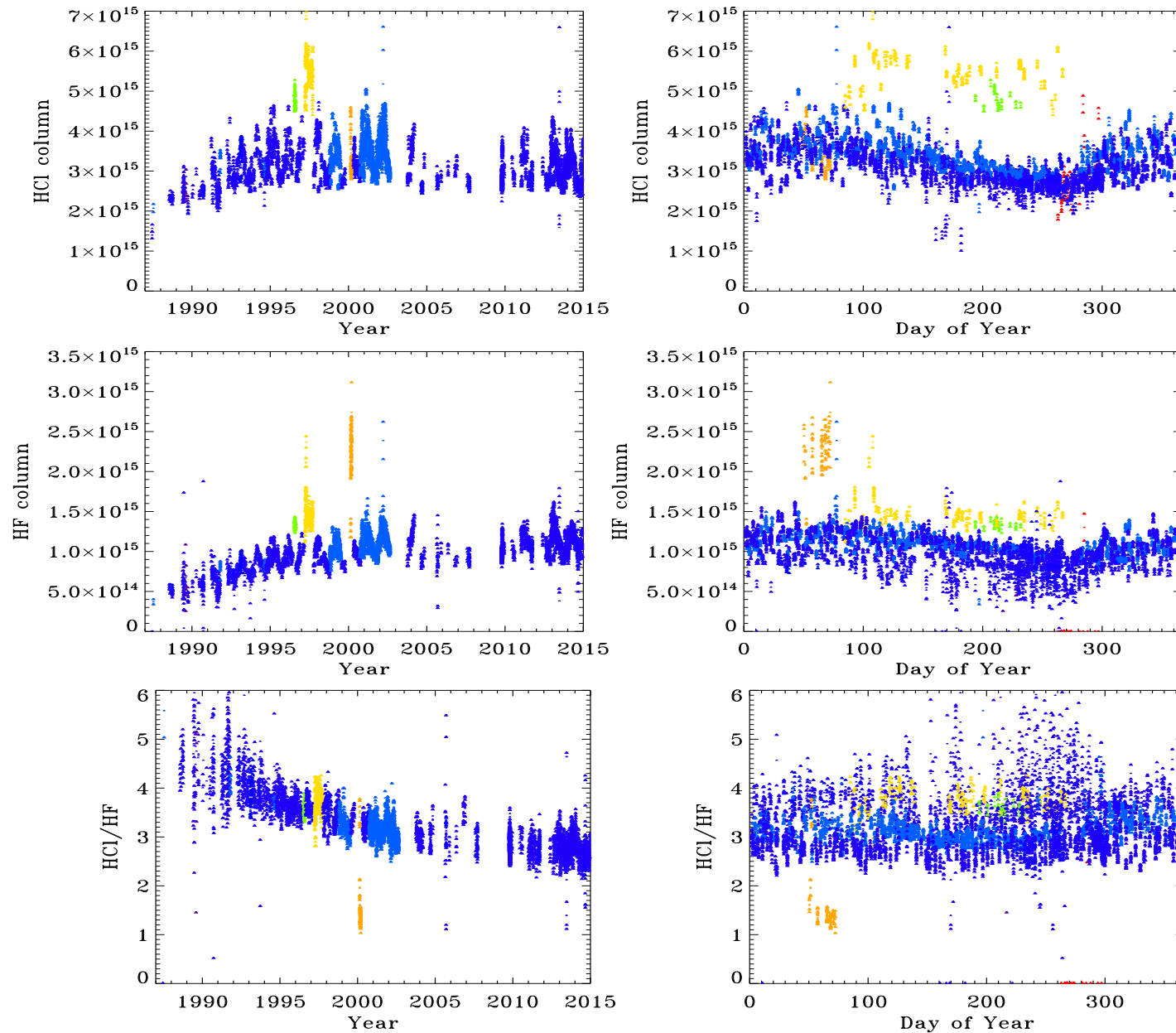
Improve accuracy/precision of retrievals:

- Wider windows
- Linelist improvements
- Develop empirical pseudo-linelist for gases poorly represented in HITRAN or completely missing (e.g. C_2H_6 , C_3H_8 , SF_6 , N_2O_5 , CH_3OH , CCl_2F_2)
- Better a priori vmr profiles

MkIV CO₂ columns



HCl and HF (color-coded by latitude)

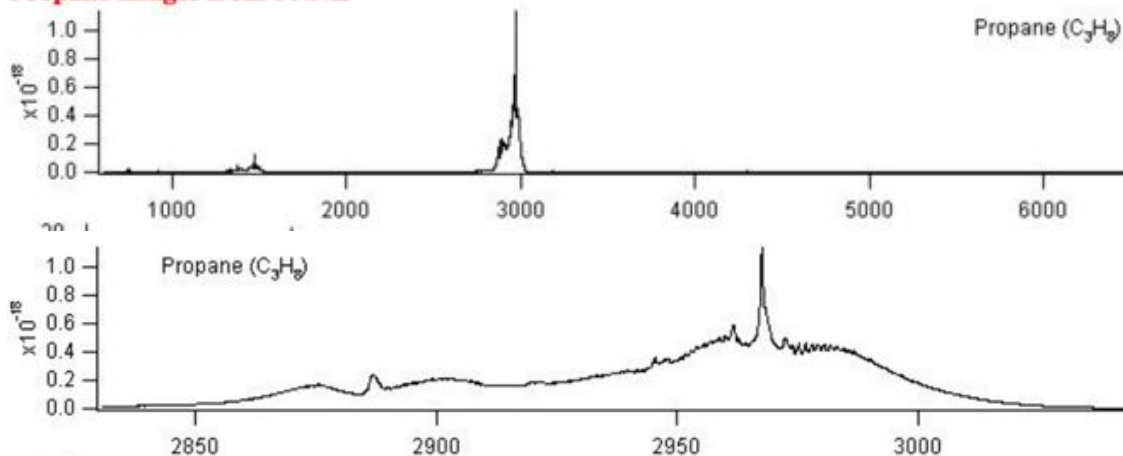


MkIV column measurements of Propane

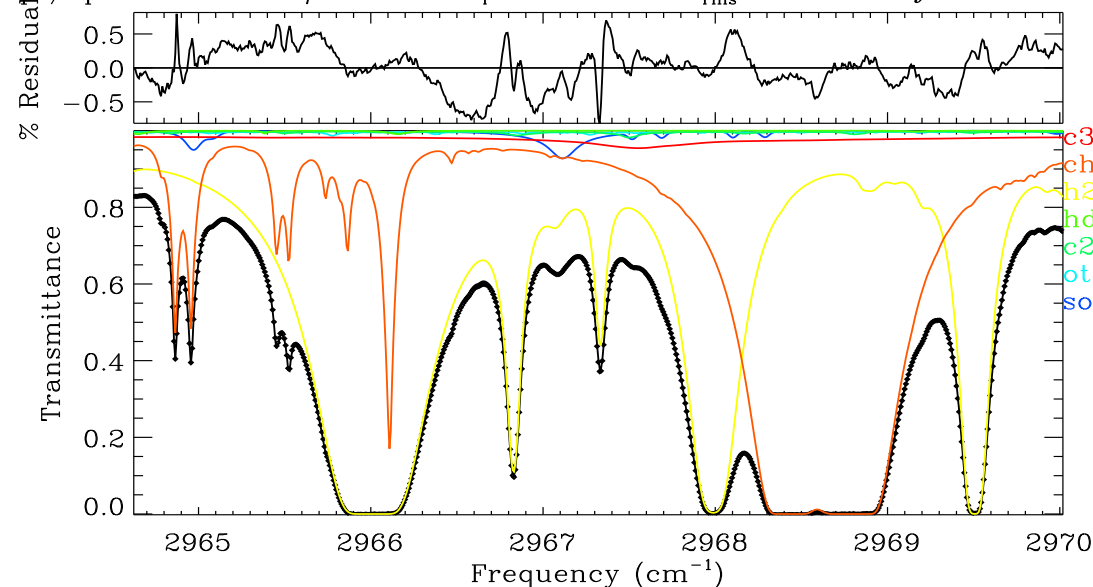
Right: PNNL lab measurements of propane. The strongest absorption is 2900-3000 cm^{-1} , especially Q-branch at 2967 cm^{-1}

Below: Fit to MkIV ground-based spectrum in vicinity of propane Q-branch, which is only 2-3% deep.

Propane images from PNNL



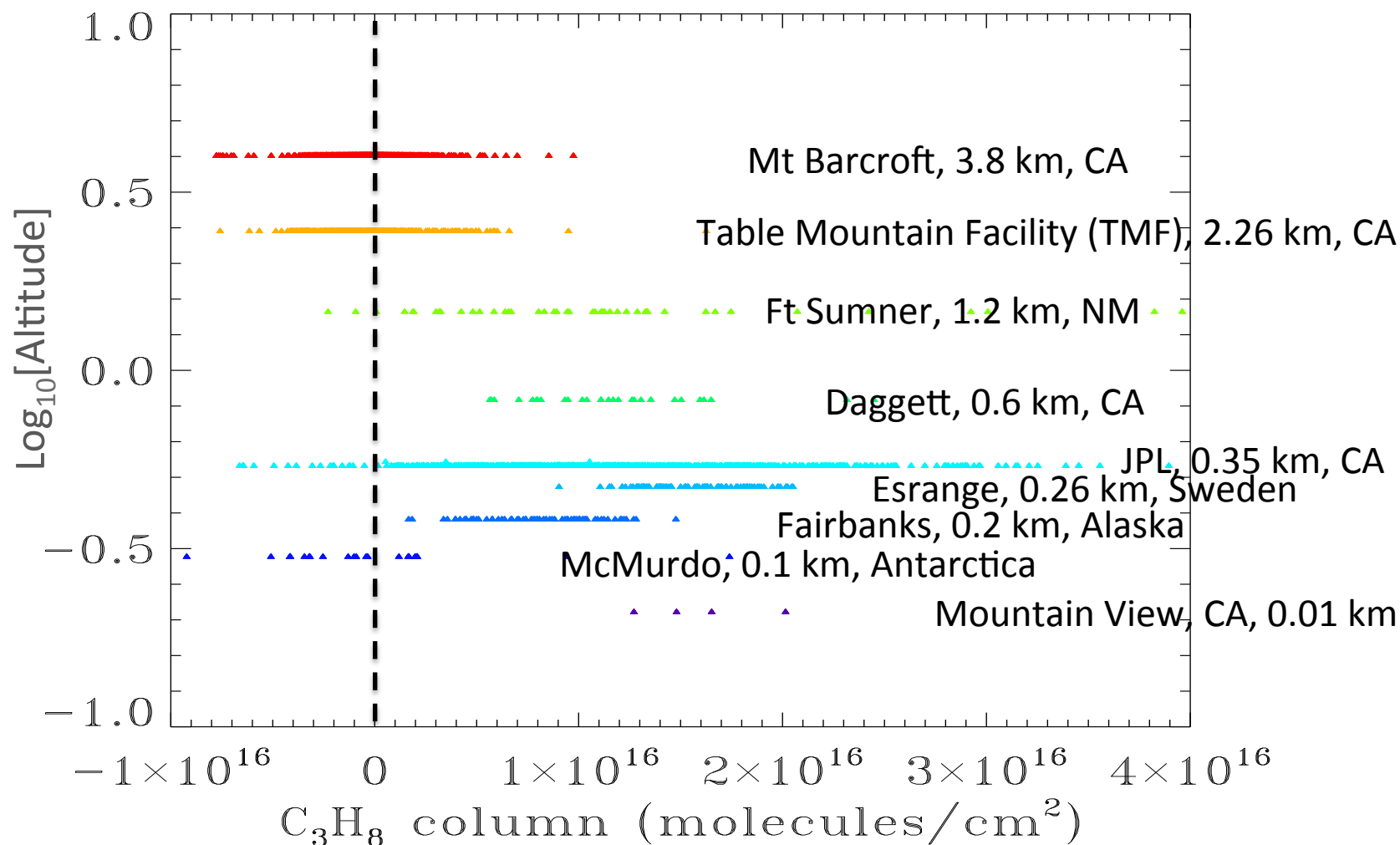
spt/zpin95103.746 $\psi = 28.58^\circ$ $Z_T = 0.30\text{km}$ $\sigma_{\text{rms}} = 0.2959\%$ $\int dz = 33.905 \pm 4.1$



C_3H_8 difficult to measure remotely:

- Generally low concentration so weak absorption
- Featureless spectrum, except for unresolved Q-branch at 2967 cm^{-1}
- No linelist in HITRAN
- This region cluttered with much stronger absorptions of H_2O , CH_4 , C_2H_6 , & solar.

Retrieved MkIV C₃H₈ columns



High altitude sites have essentially zero propane, implying that it is a PBL pollutant.

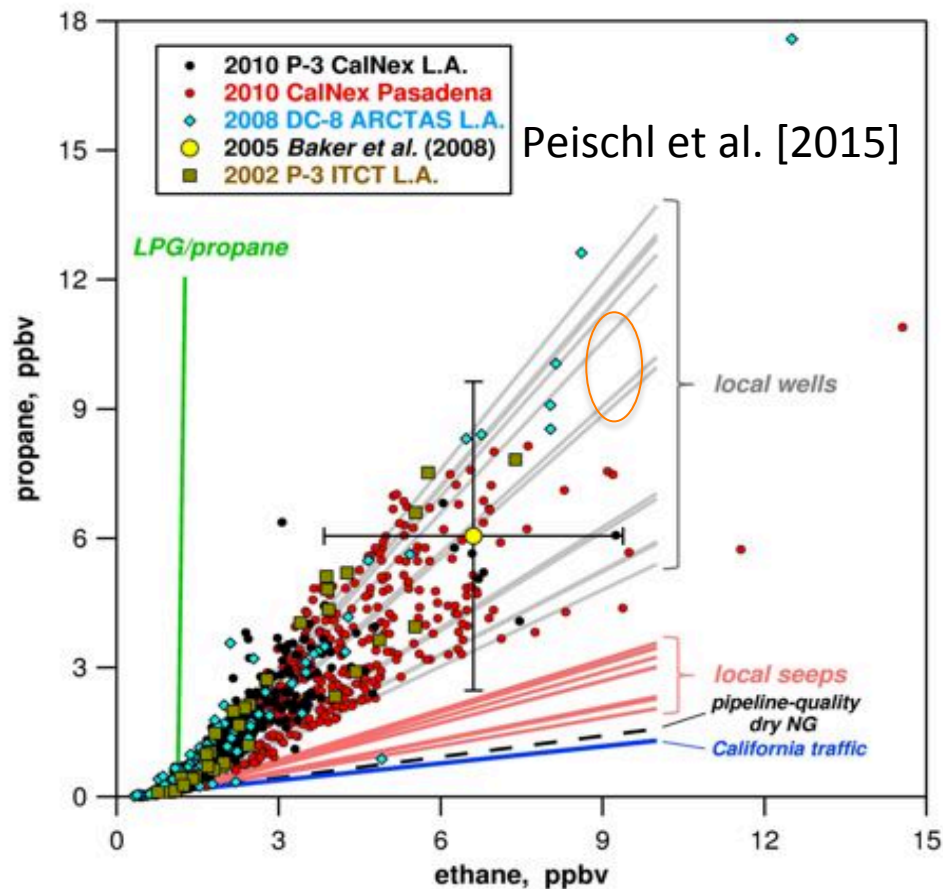
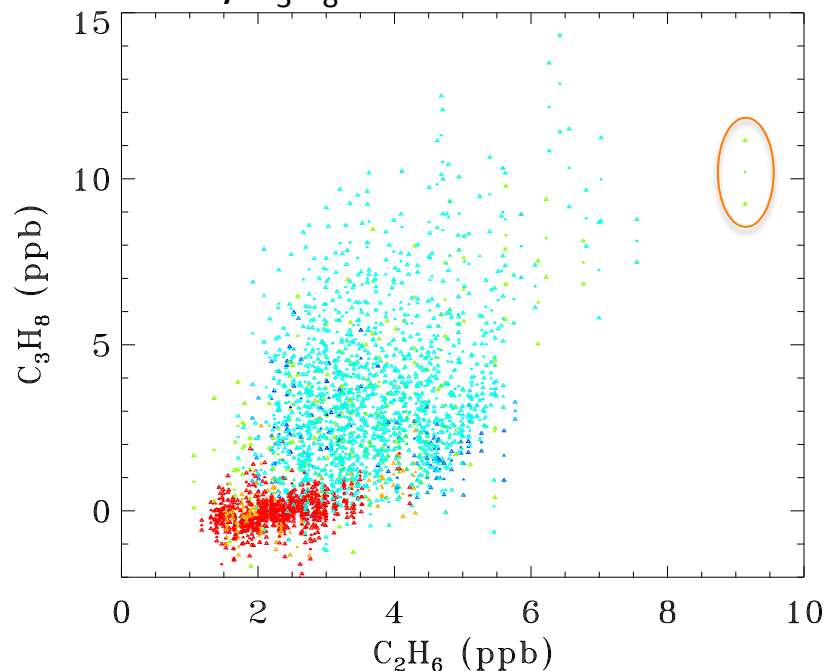
McMurdo, Antarctica, also has zero propane, despite being at sea-level.

JPL generally has the most propane, although it can occasionally be high in Ft Sumner

$C_3H_8-C_2H_6$: Comparison with in situ measurements

Figure (right) from Peischl [2015] shows in situ measurements of C_3H_8 over the LA basin, plotted versus C_2H_6 .

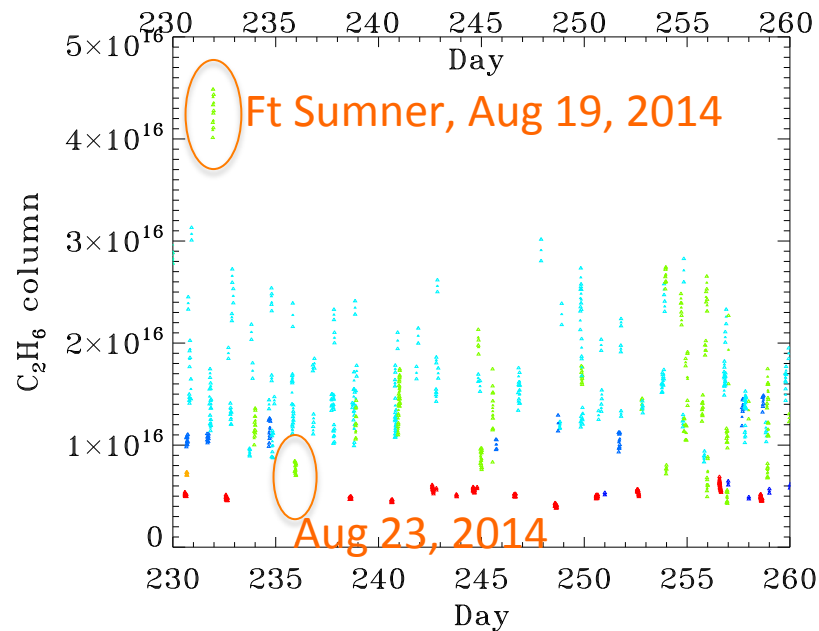
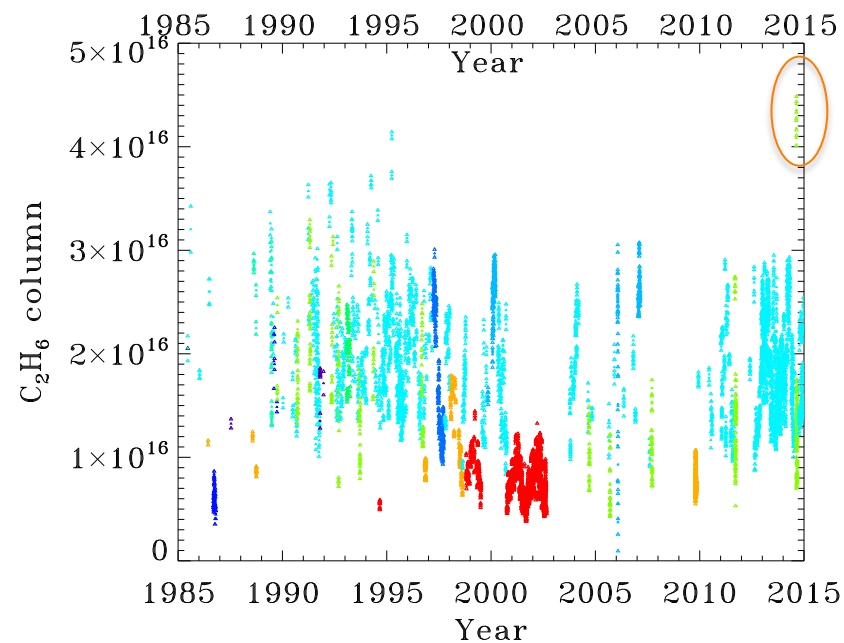
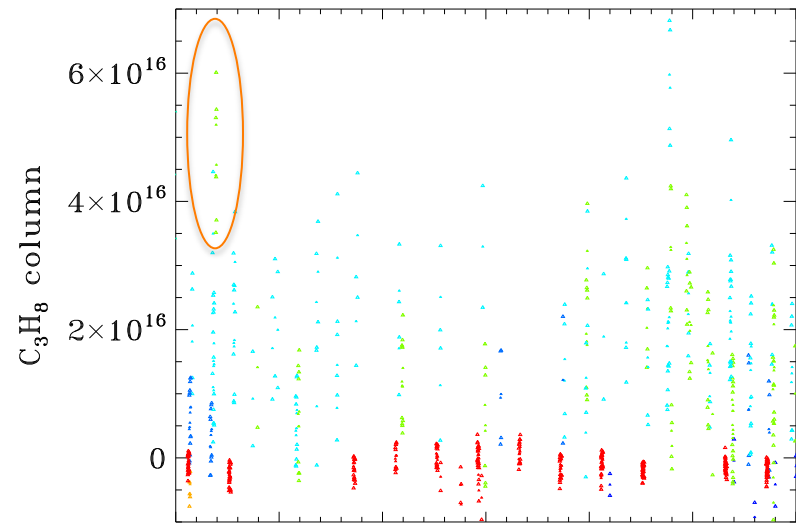
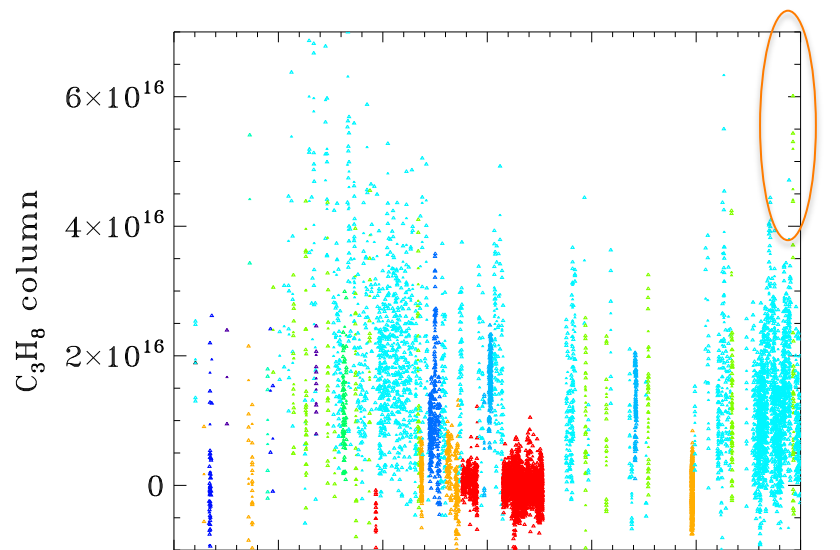
Figure below is MkIV $C_3H_8-C_2H_6$ correlation. Columns converted to ppb by assuming uniformity in lowest 3 km (PBL). High altitude measurements (red, orange, green) show very C_3H_8 .



Peischl et al. [2015]

The retrieved C_3H_8 columns appear reasonable. Agree with in situ measurements over LA basin. Close to zero in the free troposphere.

MkIV C_3H_8 and C_2H_6 time series



HYSPLIT back-trajectory for Aug 19, 2014



Three back-trajectories, encompassing the 2 hour observation period on Aug 19, 2014, the day of the anomalously high C_2H_6 and C_3H_8 . The sampled air mass had been over SE New Mexico 24 hours earlier.

Google Earth Images of origin of HYSPLIT back-trajectory

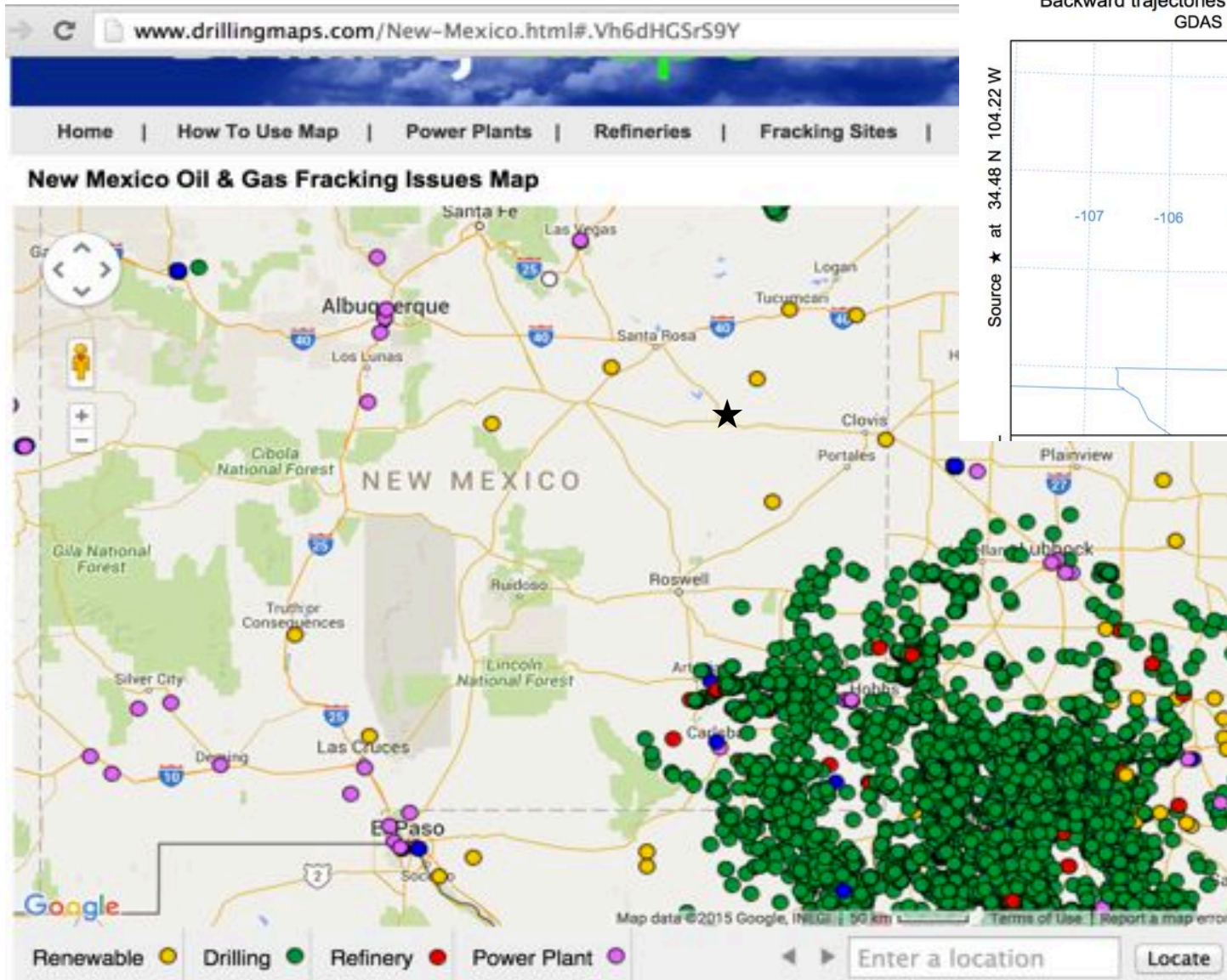


Left: Zoom into Google Earth image at end of blue back-trajectory reveals thousands of regularly-spaced squares in an otherwise desolate landscape,

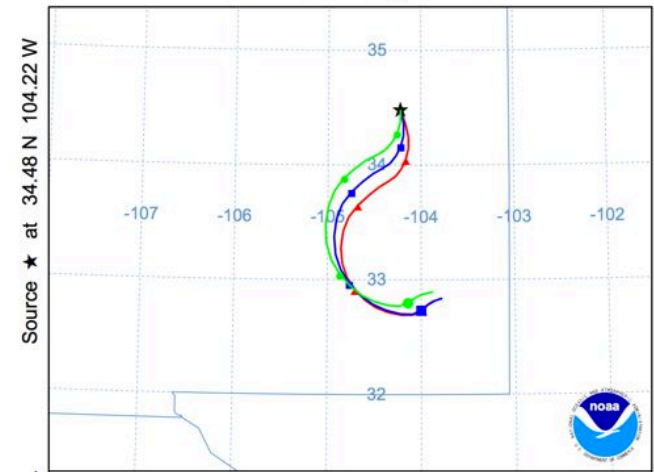
Right: Further zooming into one of the many squares reveals an oil rig pump.



Drilling Maps

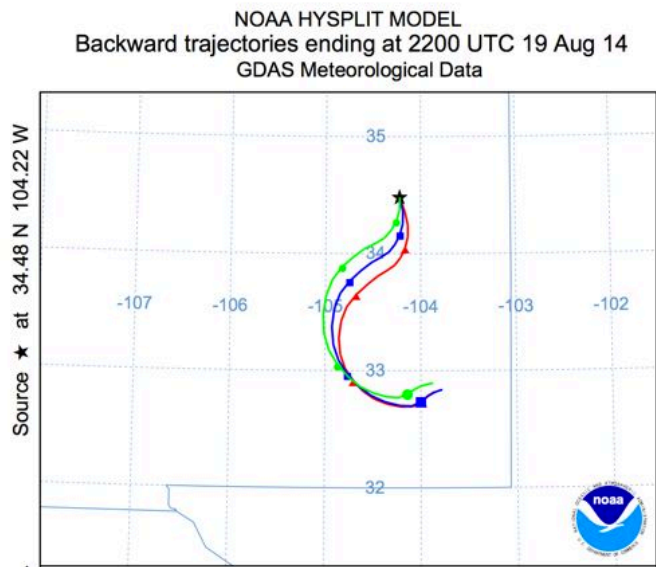


NOAA HYSPLIT MODEL
Backward trajectories ending at 2200 UTC 19 Aug 14
GDAS Meteorological Data

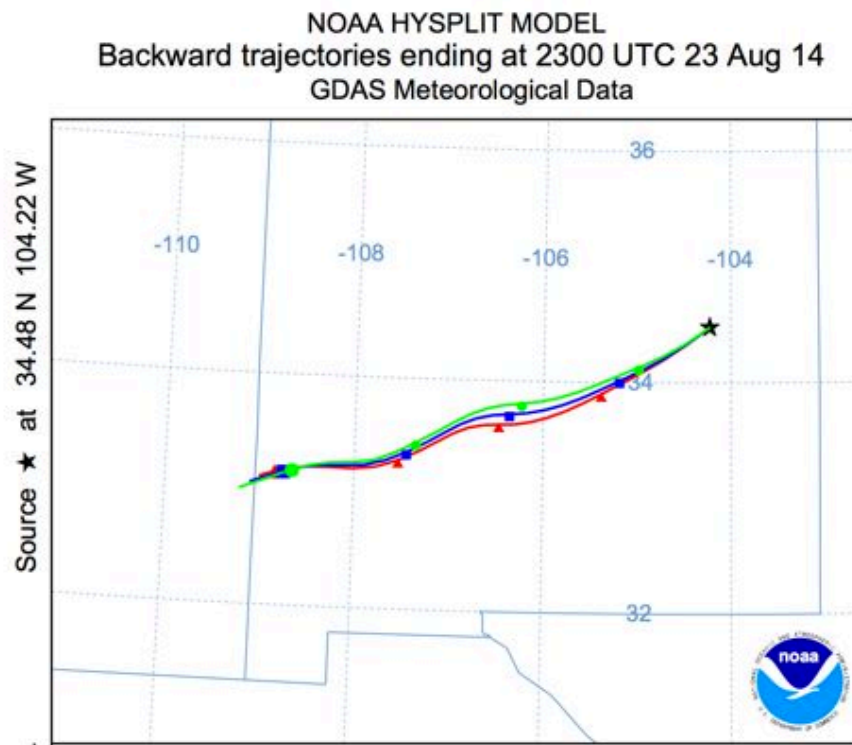


The most exploited oil and gas field in the US lies in SE New Mexico and West Texas

Comparison of back-trajectories



Aug 19 back-trajectory shows slow-moving airmass that was over SE New Mexico 24 hours prior to the observation of anomalously high C_3H_8 and C_2H_6 .



Aug 23 back-trajectory shows fast-moving airmass from SW New Mexico. This situation is much more typical for sunny days in Ft Sumner.

No other gases exhibited an anomaly on Aug 19, not even CH_4 .

MOHAVE Campaign at TMF

Atmos. Meas. Tech., 4, 2579–2605, 2011
www.atmos-meas-tech.net/4/2579/2011/
doi:10.5194/amt-4-2579-2011
© Author(s) 2011. CC Attribution 3.0 License.



Measurements of Humidity in the Atmosphere and Validation Experiments (MOHAVE)-2009: overview of campaign operations and results

T. Leblanc¹, T. D. Walsh¹, I. S. McDermid¹, G. C. Toon², J.-F. Blavier², B. Haines², W. G. Read², B. Herman², E. Fetzer², S. Sander², T. Pongetti², D. N. Whiteman³, T. G. McGee³, L. Twigg³, G. Sumnicht³, D. Venable⁴, M. Calhoun⁴, A. Dirisu⁵, D. Hurst⁶, A. Jordan⁶, E. Hall⁶, L. Miloshevich⁷, H. Vömel⁸, C. Straub⁹, N. Kampfer⁹, G. E. Nedoluha¹⁰, R. M. Gomez¹⁰, K. Holub¹¹, S. Gutman¹¹, J. Braun¹², T. Vanhove¹², G. Stiller¹³, and A. Hauchecorne¹⁴

MkIV was one of 6 instruments measuring water vapor above TMF in Oct 2009 over a 3-week period.

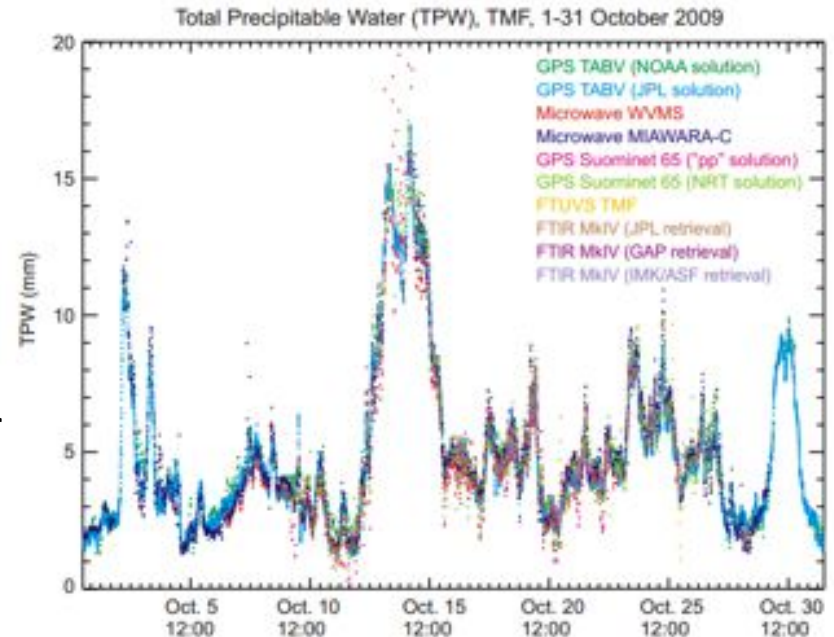
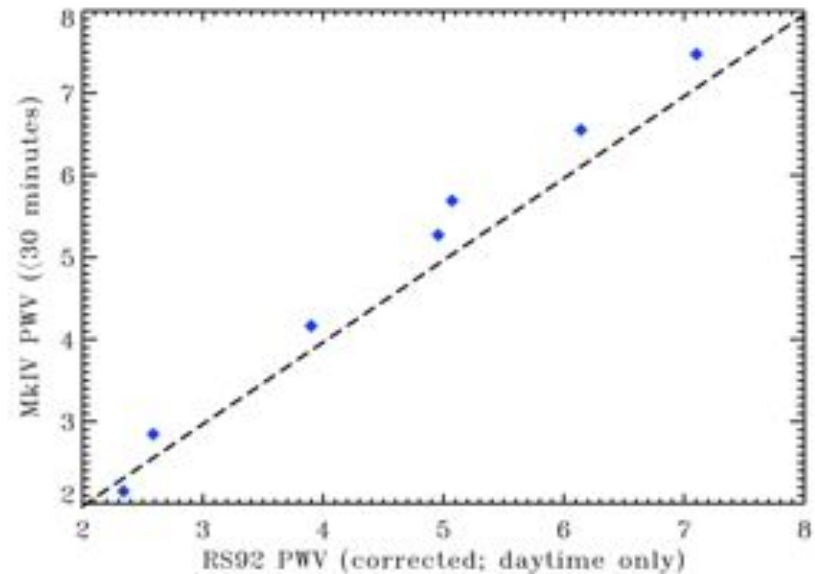
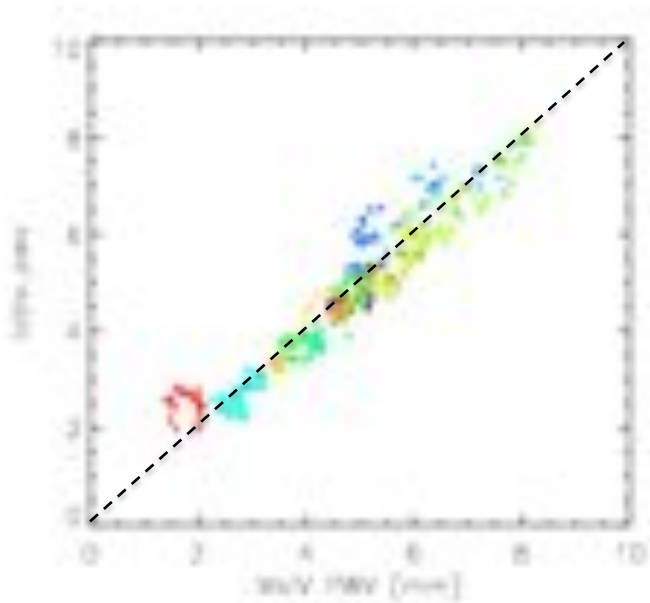
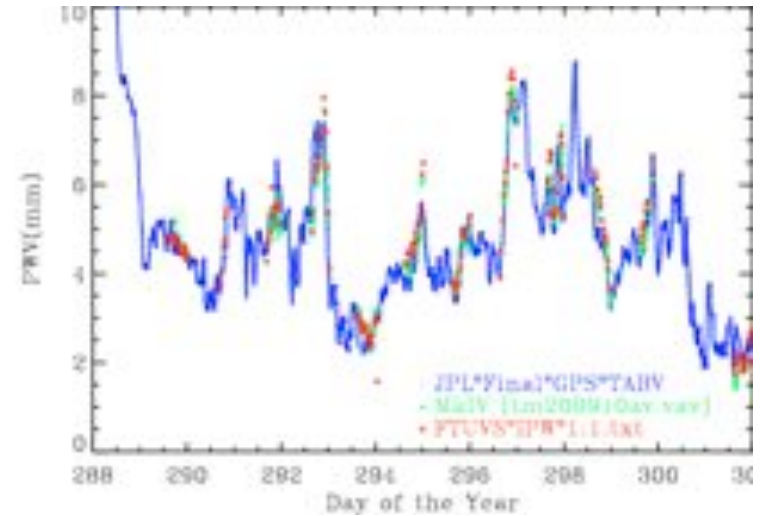
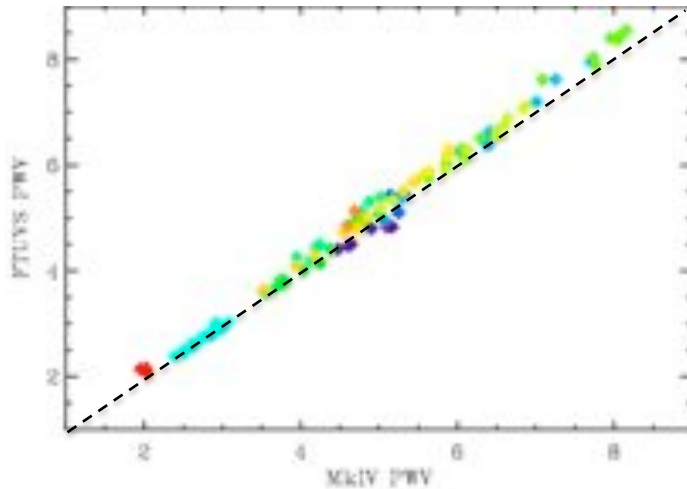


Fig. 14. Time series (1–31 October 2009) of the Total Precipitable Water datasets obtained from the two GPS, two microwave radiometers, and two Fourier Transform Spectrometers deployed at TMF during MOHAVE-2009. Sampling interval varies between 10-min and 45-min.

MOHAVE Campaign at TMF



Excellent agreement between very different techniques.

Summary & Conclusions

MkIV is a unique instrument (very broad spectral coverage, no NDACC filters)

The ground-based dataset is also unique

- Covers 12 very different sites
- GFIT analysis (profile scaling retrieval, ATM_2015 linelist)

Unfortunately, uniqueness is not an attribute that endears modelers to your data.

Rather than simply mimic a NDACC primary site, I have tried to to exploit the unique aspects of the MkIV instrument

- Wide simultaneous spectral coverage
- Existence of exo-atmospheric solar spectra (from balloon flights)
- Wide variety of measurement conditions

to perform investigations that benefits the NDACC-IRWG as a whole.

Thanks to NASA Upper Atmosphere Research Program for continued support.

I appreciate the opportunity to speak at the NDACC Steering Committee Mtg.

H₂O Spectroscopy Problems

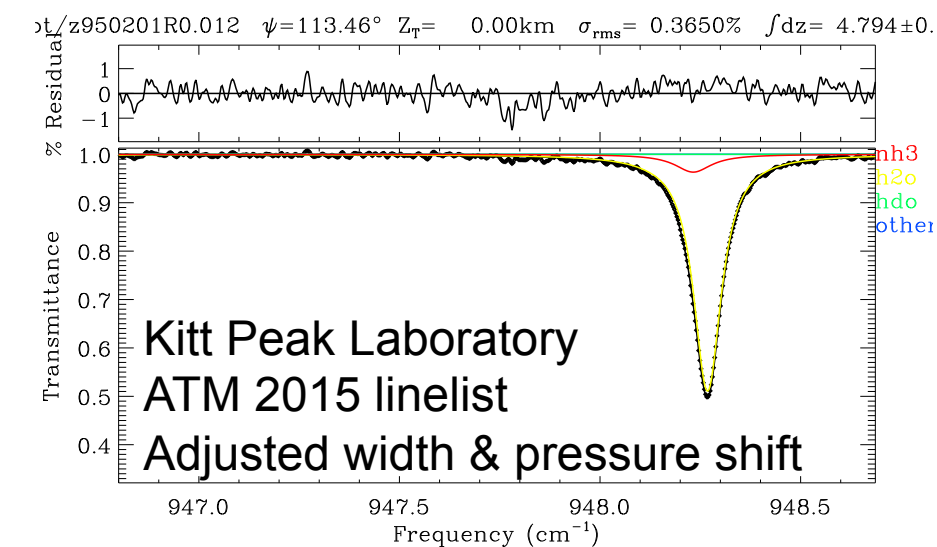
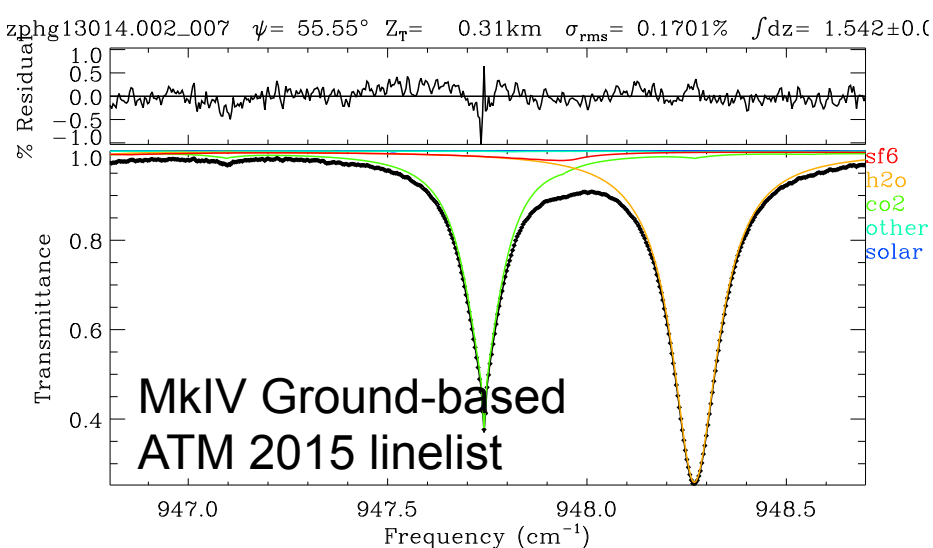
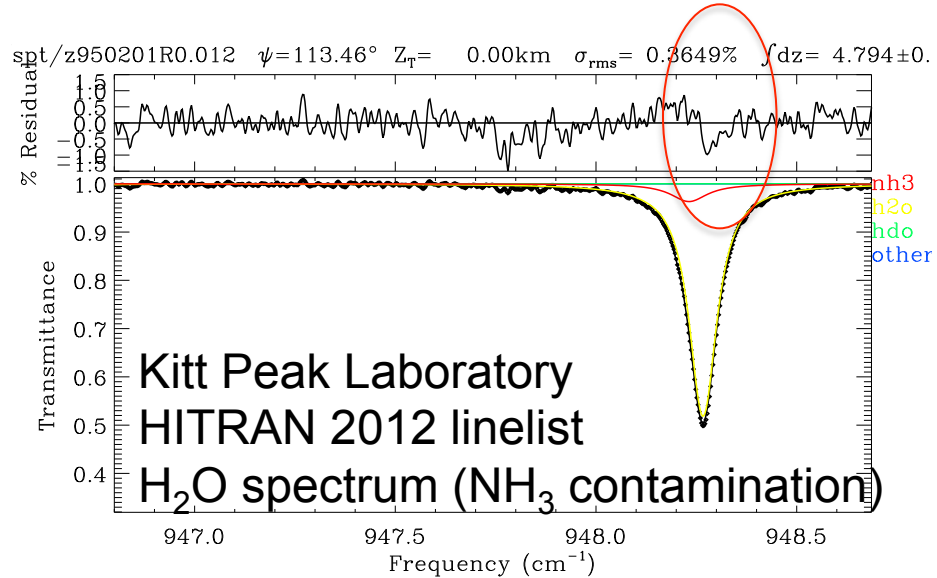
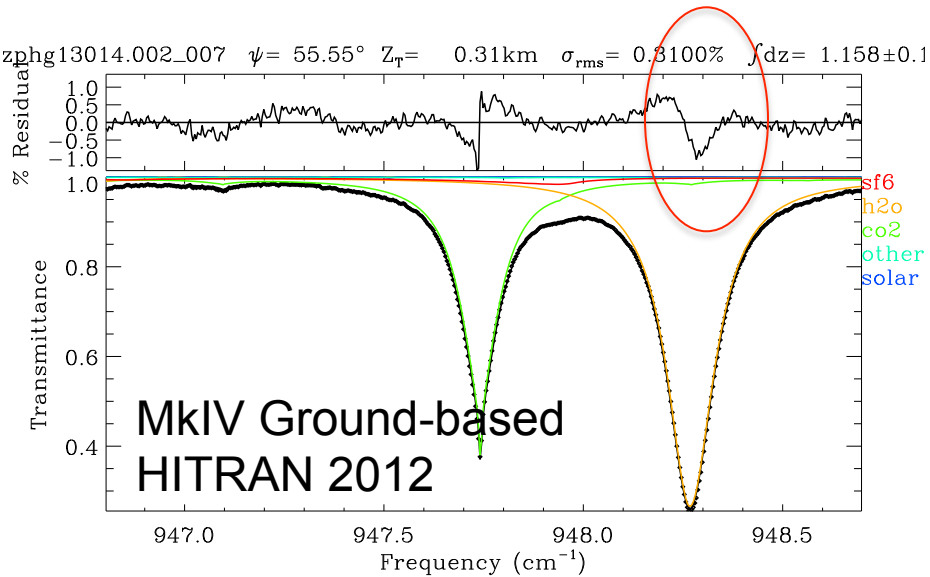
We all know that H₂O is important as a greenhouse gas.

But H₂O spectroscopy is also important since H₂O lines are ubiquitous in the IR and often overlap much weaker lines of gases of interest (e.g. HF, H₂CO, SF₆, HCN)

A 1% error in the calculated absorption of a H₂O line can easily cause a 5% error in the retrieved column of the weak overlapping gas of interest.

Additionally, spectroscopic inconsistencies can cause/mask biases between different instruments operating in different spectral regions.

MkIV solar & Kitt Peak lab spectra: SF₆ window



Minor modification to interfering H₂O line spectroscopy causes 35% increase in retrieved SF₆ and factor ~2 reduction in uncertainty.

Consistency of H₂O windows using

different linelists

hitran_2012 linelist

Window	Bias	χ^2
h2o_841	0.98744 ± 0.00976	2.32972
h2o_1111	0.99840 ± 0.01006	3.31236
h2o_1117	1.11458 ± 0.04841	2.71080
h2o_1121	1.02072 ± 0.01315	1.88117
h2o_1959	1.03246 ± 0.01273	1.19943
h2o_2819	1.03731 ± 0.01339	3.37359
h2o_2871	1.05095 ± 0.01730	0.90271
h2o_3001	0.99439 ± 0.04809	0.60583
h2o_3019	1.02041 ± 0.01914	1.10095
h2o_3155	1.05087 ± 0.01181	1.09150
h2o_3163	1.00991 ± 0.01441	1.45657
h2o_3205	1.00008 ± 0.00771	1.52544
h2o_4056	0.93535 ± 0.01210	1.72251
h2o_4537	0.98502 ± 0.01036	1.62322
h2o_4543	1.00994 ± 0.01677	1.06846
h2o_4552	1.00616 ± 0.01133	1.99484
h2o_4556	0.99082 ± 0.01356	0.36957
h2o_4565	0.98195 ± 0.01031	0.82703
h2o_4570	1.00772 ± 0.01151	0.78087
h2o_4571	0.99534 ± 0.01700	0.86081
h2o_4576	0.99435 ± 0.01375	1.15507
h2o_4598	0.99759 ± 0.01292	0.66952
h2o_4611	0.97943 ± 0.00987	2.99050
h2o_4622	0.99403 ± 0.01457	1.20233
h2o_4631	1.00508 ± 0.01142	1.18690
h2o_4699	0.99237 ± 0.01019	2.79317
h2o_4734	1.01006 ± 0.01433	1.50251
h2o_4761	1.00641 ± 0.01604	1.12048
th2o_4054	1.08972 ± 0.01549	3.99992
th2o_4255	1.02332 ± 0.03141	0.89346
th2o_4325	0.86174 ± 0.01747	3.51775
th2o_4493	0.95047 ± 0.01342	1.84255
th2o_4516	1.03158 ± 0.02760	1.07099
th2o_4524	1.00054 ± 0.01192	2.35515
th2o_4633	1.01840 ± 0.01325	1.50168

Window-to-window biases in H₂O columns retrieved from MkIV data

Left: Using HITRAN 2012

Right: Using modified linelist

Certain windows have strong biases using HITRAN linelist.

Atm_2015 linelist based on Toth [2003] modified based on fits to Kitt Peak lab spectra.

Kitt Peak lab spectra do not cover all these windows simultaneously. So MkIV solar spectra used to impose consistency between MIR and NIR regions.

atm_2015 linelist

Window	Bias	χ^2
h2o_841	1.00141 ± 0.00994	2.02747
h2o_1111	1.02587 ± 0.01132	5.16800
h2o_1117	1.02202 ± 0.01360	10.32960
h2o_1121	1.03338 ± 0.01468	6.25062
h2o_1959	1.00286 ± 0.01160	1.24620
h2o_2819	1.01113 ± 0.01322	2.97597
h2o_2871	1.00122 ± 0.01663	0.76769
h2o_3001	0.98423 ± 0.03505	0.86576
h2o_3019	1.01065 ± 0.02002	1.12680
h2o_3155	1.03863 ± 0.01139	1.08713
h2o_3163	1.01844 ± 0.01339	1.28314
h2o_3205	0.97668 ± 0.00832	1.99347
h2o_4056	0.99507 ± 0.01333	1.82023
h2o_4537	0.99345 ± 0.01023	1.25667
h2o_4543	0.99117 ± 0.01360	1.33326
h2o_4552	0.98836 ± 0.01270	1.50336
h2o_4556	1.00128 ± 0.01077	0.74845
h2o_4565	1.00369 ± 0.00957	1.01293
h2o_4570	0.98864 ± 0.01231	1.29895
h2o_4571	0.98601 ± 0.01624	0.74570
h2o_4576	1.00039 ± 0.01144	1.11882
h2o_4598	0.99855 ± 0.01011	1.42424
h2o_4611	0.98757 ± 0.01001	3.15451
h2o_4622	1.00133 ± 0.01150	1.66678
h2o_4631	0.99724 ± 0.00995	2.01445
h2o_4699	0.98716 ± 0.00947	4.98491
h2o_4734	0.98949 ± 0.01078	2.23066
h2o_4761	1.00166 ± 0.01131	1.78963
th2o_4054	1.00698 ± 0.01127	3.78947
th2o_4255	0.99518 ± 0.01655	1.80179
th2o_4325	1.01807 ± 0.01448	4.22593
th2o_4493	0.99245 ± 0.01088	2.41777
th2o_4516	1.00375 ± 0.01743	1.01267
th2o_4524	0.99175 ± 0.00959	2.44873
th2o_4633	0.99534 ± 0.01231	1.05554

MkIV H₂O windows

h2o_841	0.98744 ± 0.00976	2.32972
h2o_1111	0.99840 ± 0.01006	3.31236
h2o_1117	1.11458 ± 0.04841	2.71080
h2o_1121	1.02072 ± 0.01315	1.88117
h2o_1959	1.03246 ± 0.01273	1.19943
h2o_2819	1.03731 ± 0.01339	3.37359
h2o_2871	1.05095 ± 0.01730	0.90271
h2o_3001	0.99439 ± 0.04809	0.60583
h2o_3019	1.02041 ± 0.01914	1.10095
h2o_3155	1.05087 ± 0.01181	1.09150
h2o_3163	1.00991 ± 0.01441	1.45657
h2o_3205	1.00008 ± 0.00771	1.52544

NDACC H₂O
Windows

h2o_4056	0.93535 ± 0.01210	1.72251
h2o_4537	0.98502 ± 0.01036	1.62322
h2o_4543	1.00994 ± 0.01677	1.06846
h2o_4552	1.00616 ± 0.01133	1.99484
h2o_4556	0.99082 ± 0.01356	0.36957

TCCON H₂O windows

h2o_4565	0.98195 ± 0.01031	0.82703
h2o_4570	1.00772 ± 0.01151	0.78087
h2o_4571	0.99534 ± 0.01700	0.86081
h2o_4576	0.99435 ± 0.01375	1.15507
h2o_4598	0.99759 ± 0.01292	0.66952
h2o_4611	0.97943 ± 0.00987	2.99050
h2o_4622	0.99403 ± 0.01457	1.20233
h2o_4631	1.00508 ± 0.01142	1.18690
h2o_4699	0.99237 ± 0.01019	2.79317
h2o_4734	1.01006 ± 0.01433	1.50251
h2o_4761	1.00641 ± 0.01604	1.12048

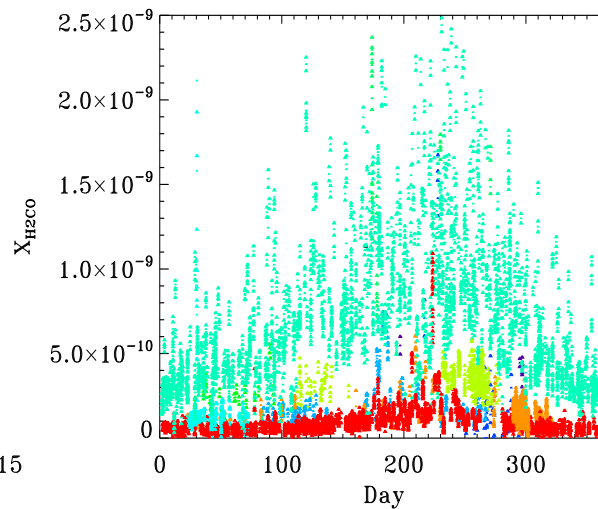
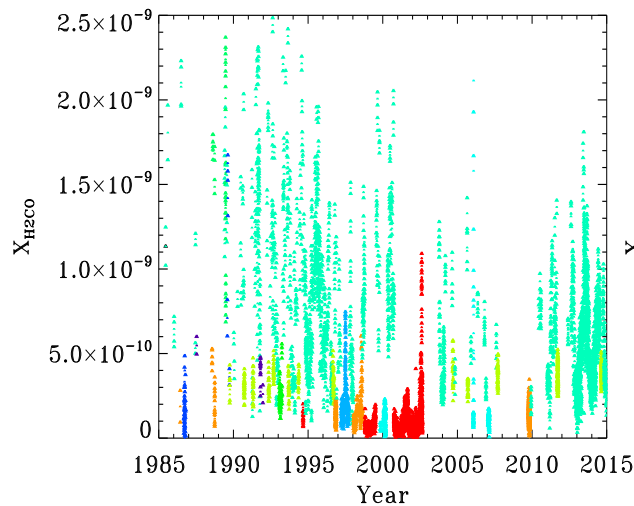
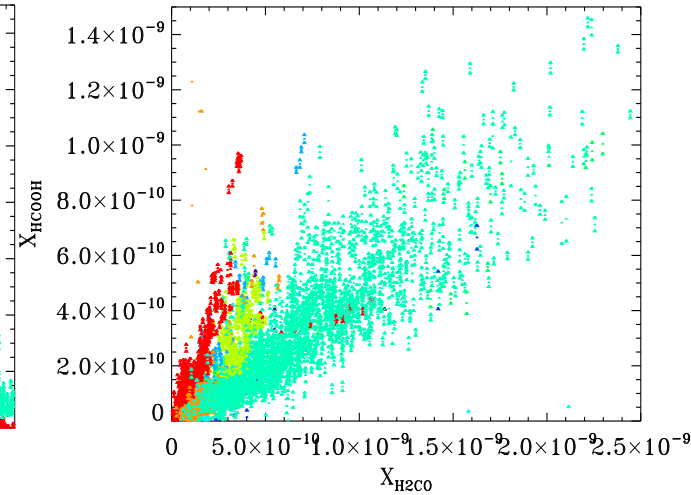
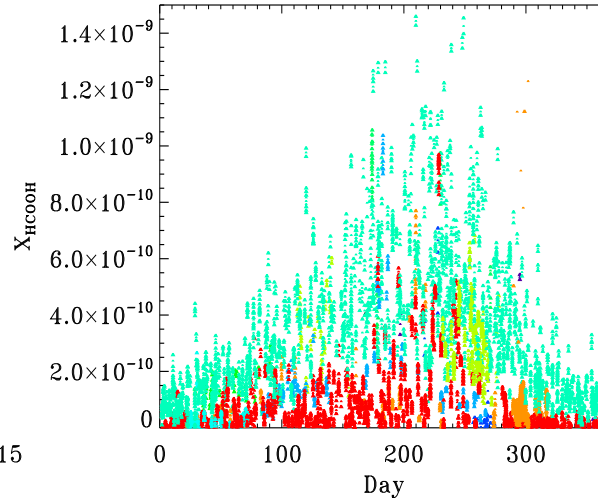
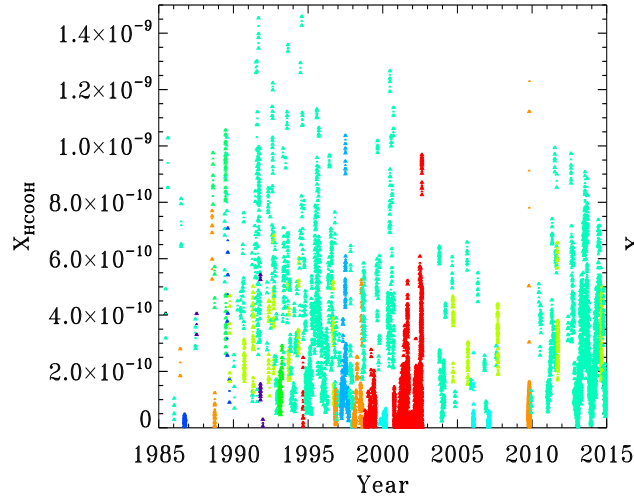
h2o_4565	1.00569 ± 0.00569	0.63439
h2o_4570	0.99501 ± 0.01057	0.61044
h2o_4571	0.99448 ± 0.01031	0.47245
h2o_4576	0.99992 ± 0.00670	0.67522
h2o_4598	1.00677 ± 0.00830	0.28215
h2o_4611	1.00343 ± 0.00567	0.97659
h2o_4622	1.01219 ± 0.00562	1.04209
h2o_4631	1.00791 ± 0.00615	0.71785
h2o_4699	1.00928 ± 0.00513	1.08487
h2o_4734	0.99855 ± 0.00838	0.50628
h2o_4761	1.00401 ± 0.00897	0.39901

Common
H₂O windows

h2o_6076	1.01386 ± 0.01279	0.82159
h2o_6099	1.03429 ± 0.01231	1.20415
h2o_6125	1.01546 ± 0.01239	0.97713
h2o_6177	1.04902 ± 0.01651	1.23276
h2o_6255	1.00312 ± 0.01641	0.72414
h2o_6301	0.97605 ± 0.00878	0.81082
h2o_6392	0.98993 ± 0.00963	0.99677
h2o_6401	0.99147 ± 0.01149	0.88970
h2o_6469	1.03598 ± 0.01123	1.00613

Consistency of H₂O windows

MkIV HCOOH and H₂CO



Both H₂CO and HCOOH are tropospheric pollutants. They decrease strongly with altitude. But H₂CO decreases more rapidly than HCOOH. So the gradient HCOOH/H₂CO increases with altitude.

Surprisingly tight, altitude-dependent, correlations are seen between HCOOH and H₂CO